Yrast spectroscopy of ^{130}Nd and evidence of a highly deformed band

D. J. Hartley, W. Reviol,* L. L. Riedinger, H. Q. Jin,† B. H. Smith,‡ N. Yoder,§ and O. Zeidan
Department of Physics and Astronomy, University of Tennessee, Knoxville, Tennessee 37996

A. Galindo-Uribarri
Physics Division, Oak Ridge National Laboratory, Oak Ridge, Tennessee 37831

D. G. Sarantites, D. R. LaFosse,‖ and J. N. Wilson¶
Chemistry Department, Washington University, St. Louis, Missouri 63130

S. M. Mullins**
Department of Nuclear Physics, Australian National University, Canberra ACT 0200, Australia
(Received 11 August 2000; published 23 January 2001)

High-spin states in ^{130}Nd were populated in the reaction ^{94}Mo(^{40}Ca,$2p2n$) at a beam energy of 180 MeV. The ground-state band has been extended to $I^{\pi}=(32^{+})$ and three side bands were observed for the first time. In addition, a weak band with a large dynamical moment of inertia was found. The moment of inertia of this sequence is similar to those of structures found to be highly deformed in heavier even-even Nd nuclei.

DOI: 10.1103/PhysRevC.63.024316 PACS number(s): 21.10.Re, 23.20.Lv, 27.60.+j

I. INTRODUCTION

The nuclei in the light rare-earth region have attracted much attention recently as a sundry of highly deformed bands have been observed. These structures typically have a quadrupole deformation parameter of $\beta_2=0.3-0.4$ (see Refs. [1,2], for example), while bands of normal deformation in the same nuclei are found to have $\beta_2=0.20-0.25$. Occupation of at least one neutron in the intruder $i_{13/2}$ orbital, the presence of highly deformed shell gaps at $N=72$, 74, and/or holes in the proton $g_{9/2}$ orbital are often cited as the primary causes of these sequences. In particular, such bands have been found in a long chain of Nd ($Z=60$) nuclei, $N=71-77$ [3–9]. As these nuclei become more neutron deficient, the neutron Fermi surface approaches midshell, and therefore creates increasingly larger ground-state deformations. Calculations from Möller and Nix [10] predict that the ground-state deformations steadily grow and peak near $N=66$ with $\beta_2=0.33$, which is as large as many of the observed highly deformed bands in the heavier Nd nuclei. Thus exploring the well-deformed, proton-rich Nd nuclei is of significant interest, especially to inquire how far below the $i_{13/2}$ orbital and the $N=72$ shell gap highly deformed bands can be observed. With this perspective, high-spin states of ^{130}Nd have been investigated and a candidate highly deformed sequence has been identified.

II. EXPERIMENTAL DETAILS

The reaction ^{94}Mo(^{40}Ca,$2p2n$) was used to populate high-spin states in ^{130}Nd. The ^{40}Ca beam was accelerated to 180 MeV by the 88-Inch Cyclotron facility located at the Lawrence Berkeley National Laboratory, and was focused onto a $\sim$0.5 mg/cm^2 self-supporting ^{94}Mo foil. The Gammasphere spectrometer [11] was used in conjunction with the selectivity of the Washington University Microball [12] to detect the emitted γ rays and charged particles, respectively. Approximately 8.3×10^8 events were recorded when at least one of the 95 CsI detectors from the Microball and at least four of the 92 Compton-suppressed Ge detectors were in prompt coincidence. Gamma rays associated with the emission of two protons (comprising $\sim$17% of the total events) were sorted into an $E_\gamma\times E_\gamma\times E_\gamma$ cube, which was analyzed with the RADWARE [13] package. Based upon the deduced coincidence relationships, a new level scheme for ^{130}Nd is proposed and shown in Fig. 1. The energies and intensities of the γ rays obtained from the present work are listed in Table I.

For determination of the spins of the observed states, an angular-dependent $E_\gamma\times E_\gamma$ matrix enabled us to perform an analysis of the directional correlation of oriented states (DCO). Specifically, gamma rays detected at angles of 31.7°, 37.4°, 142.6°, or 148.3° (symmetric forward and backward angles denoted hereafter as FB) were projected along one axis whereas coincident γ rays detected at 90° were projected along the other axis. The DCO ratio is then defined by the expression

*Present address: Chemistry Department, Washington University, St. Louis, MO 63130.
†Present address: NASA Ames Research Laboratory, M/S T27A-1, Moffett Field, CA 94035.
‡Present address: Viridien Technologies, Inc., Boxborough, MA 01719.
§Present address: Dallas Theological Seminary, Dallas, TX 75204.
‖Present address: Department of Physics and Astronomy, State University of New York at Stony Brook, Stony Brook, NY 11794.
¶Present address: Niels Bohr Institute, Copenhagen DK-2100, Denmark.
**Present address: National Accelerator Center, P.O. Box 72, Faure ZA-7131, South Africa.

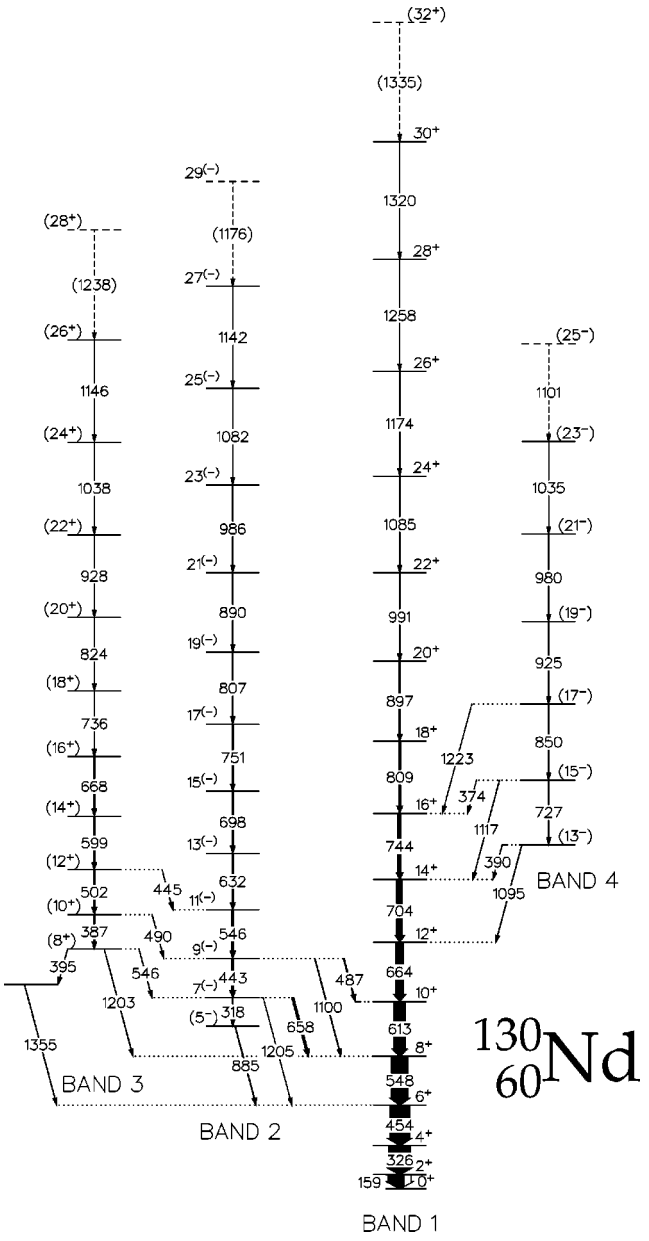

FIG. 1. The level scheme for ^{130}Nd. The width of the arrows is proportional to the relative intensity of the transition. Tentative transitions are denoted by dashed lines. Spin and parity assignments are explained in the text.

$$R_{DCO}=\frac{I_{\gamma_1}(\text{at FB; in coincidence with } \gamma_2 \text{ at } 90°)}{I_{\gamma_1}(\text{at } 90°\text{; in coincidence with } \gamma_2 \text{ at FB})},$$

where I_{γ_1} is the intensity of the γ ray of interest and γ_2 is the gating transition. Expected DCO ratios for pure dipole ($M1$ and $E1$) and quadrupole ($E2$) transitions are 0.5 and 1.0, respectively, when the gating transition is a stretched quadrupole ($\Delta I=2$). Results of the DCO analysis are given in Table I. Weak transitions above states of determined spin, where reliable DCO ratios could not be calculated, were assigned multipolarities assuming that normal band characteristics persist.

TABLE I. Data for levels and gamma rays in ^{130}Nd.

I_i^{π} [a]	E_{level} (keV)	E_γ (keV) [b]	I_γ [c]	DCO	Multipolarity
		Band 1			
2^+	158.6	158.6		0.98(4)	$E2$
4^+	484.8	326.2	$\equiv 100$	1.02(2)	$E2$
6^+	939.1	454.3	92(4)	1.02(2)	$E2$
8^+	1486.6	547.5	77(3)	0.95(3)	$E2$
10^+	2099.8	613.2	54(3)	1.00(3)	$E2$
12^+	2763.8	664.0	38(2)	1.00(4)	$E2$
14^+	3468.0	704.2	26(1)	1.03(5)	$E2$
16^+	4211.5	743.5	14.8(8)	1.00(9)	$E2$
18^+	5020.8	809.3	9.3(6)	0.9(1)	$E2$
20^+	5918.2	897.4	5.2(4)	1.1(1)	$E2$
22^+	6909.1	990.9	2.7(3)		$(E2)$
24^+	7993.8	1084.7	1.4(2)		$(E2)$
26^+	9167.4	1173.6	0.6(1)		$(E2)$
28^+	10425	1258	<0.5		$(E2)$
30^+	11745	1320	<0.5		$(E2)$
(32^+)	(13080)	(1335)	<0.5		$(E2)$
		Band 2			
(5^-)	1825.7	885.5	3.0(4)		$(E1)$
$7^{(-)}$	2144.1	318.4	2.7(2)		$(E2)$
		657.5	9.6(6)	0.55(5)	$(E1)$
		1205.4	1.0(1)		$(E1)$
$9^{(-)}$	2587.0	442.9	10.2(6)	0.96(9)	$E2$
		486.7	4.5(4)	0.5(1)	$(E1)$
		1100.0	2.7(3)		$(E1)$
$11^{(-)}$	3133.0	546.0	8.8(8)	1.0(1)	$E2$
$13^{(-)}$	3764.5	631.5	7.3(6)	1.0(1)	$E2$
$15^{(-)}$	4462.8	698.3	5.6(4)		$(E2)$
$17^{(-)}$	5213.4	750.6	4.9(4)		$(E2)$
$19^{(-)}$	6020.6	807.2	2.4(3)		$(E2)$
$21^{(-)}$	6910.2	889.6	1.3(2)		$(E2)$
$23^{(-)}$	7896.4	986.2	0.6(1)		$(E2)$
$25^{(-)}$	8978	1082	<0.5		$(E2)$
$27^{(-)}$	10120	1142	<0.5		$(E2)$
(29^-)	(11296)	(1176)	<0.5		$(E2)$
		Band 3			
(8^+)	2689.6	545.9	1.3(2)		$(E1)$
		1203.0	1.7(2)		$(M1/E2)$
		395.2	1.5(2)		
(10^+)	3076.3	386.7	4.7(4)		$(E2)$
		489.5	1.4(2)		$(E1)$
(12^+)	3578.6	502.3	6.7(6)		$(E2)$
		444.7	1.5(2)		$(E1)$
(14^+)	4177.6	599.0	5.3(5)		$(E2)$
(16^+)	4845.9	668.3	4.6(4)		$(E2)$
(18^+)	5582.3	736.4	2.8(3)		$(E2)$
(20^+)	6406.5	824.2	2.0(2)		$(E2)$
(22^+)	7334.9	928.4	1.1(1)		$(E2)$
(24^+)	8372.8	1037.9	0.6(1)		$(E2)$
(26^+)	9519	1146	<0.5		$(E2)$
(28^+)	(10757)	(1238)	<0.5		$(E2)$

TABLE I. *(Continued).*

I_i^{π} [a]	E_{level} (keV)	E_γ (keV) [b]	I_γ [c]	DCO	Multipolarity
		Band 4			
(13^-)	3858.1	390.1	1.7(2)		$(E1)$
		1094.7	2.0(2)		$(E1)$
(15^-)	4585.2	727.1	1.4(2)		$(E2)$
		373.8	1.1(1)		$(E1)$
		1117.3	1.7(2)		$(E1)$
(17^-)	5435.2	850.0	2.2(2)		$(E2)$
		1223.3	1.0(1)		$(E1)$
(19^-)	6360.0	924.8	1.8(2)		$(E2)$
(21^-)	7340.4	980.4	1.1(1)		$(E2)$
(23^-)	8375	1035	<0.5		$(E2)$
(25^-)	(9476)	(1101)	<0.5		$(E2)$

[a]Spin and parity of the initial state.

[b]Uncertainties in E_γ are 0.2 keV for most transitions, except for relatively weak transitions which are 0.5 keV.

[c]Relative intensity of the transition where $I_\gamma(326.2) \equiv 100$.

III. THE LEVEL SCHEME

Prior to our work, only the ground-state band had been observed in ^{130}Nd [14]. The present data enabled us to extend this band from $I^\pi = 24^+$ to (32^+) as shown in Fig. 1, where the structure is labeled as band 1. A spectrum of the ground-state band is given in Fig. 2(a), which is a result of summing all coincident spectra produced by double-gating on every combination of γ rays above the 10^+ state. For the transitions below the 20^+ level, DCO ratios were obtained and confirmed the $E2$ nature of the γ rays (see Table I). The E_{4^+}/E_{2^+} ratio is equal to 3.06, suggesting that ^{130}Nd is a good rotor as the rigid body value of this ratio is 3.33. The quadrupole deformation is estimated to be $\beta_2 = 0.304$ from the energy of the 2^+ state by using Grodzins' empirical formula [15]. A slightly lower deformation of $\beta_2 = 0.290$ is obtained when using Raman's empirical formula [16]. Both values are in good agreement with the calculations of Möller and Nix [10] ($\beta_2 = 0.311$) as well as a standard total Routhian surface (TRS) [17] calculation ($\beta_2 = 0.296$). Note that these β_2 values are near the measured deformations of the highly deformed bands in the region.

Band 2 is the strongest side band observed in ^{130}Nd as indicated in Table I and a spectrum of the sequence is displayed in Fig. 2(b). A DCO ratio of 0.55(4) was measured for the 657.5 keV linking transition from the state at 2144.1 keV in band 2 to the 8^+ state of the ground-state structure, implying a change in spin of one unit of $\hbar$. An $I \rightarrow I-1$ assignment of this γ ray would suggest that the 1205.4 keV transition, which depopulates the same state (see Fig. 1), has an $E3$ or $M3$ multipolarity. Transitions with these high multipolarities are expected to have relatively long life times that would not be observed in prompt spectroscopy. If instead an $I \rightarrow I+1$ assignment is given to the 657.5 keV γ ray, the 1205.4 keV transition would also have a dipole character. This latter scenario is much more likely than the former, thus the state at 2144.1 keV has been assigned a spin of $I = 7$. However, a firm parity assignment cannot be made for this state or band 2. Systematically, the lowest-energy side bands in even-even Nd nuclei have been given negative parity [6,18]; therefore, band 2 is also tentatively assigned odd parity.

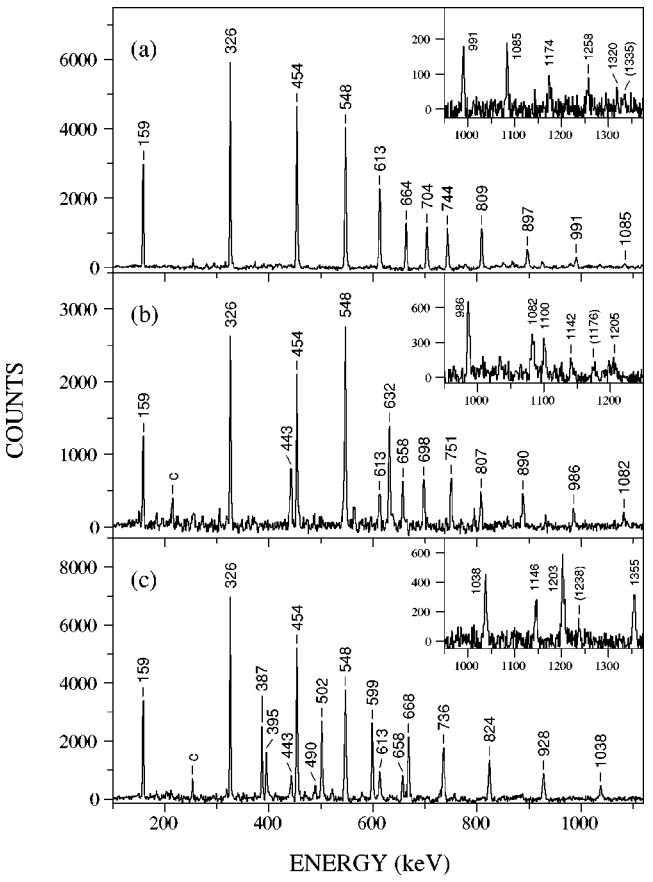

FIG. 2. (a) Spectrum of the ground-state band (band 1) in ^{130}Nd. The spectrum is a result of summing the coincidence spectra generated by double-gating on all possible combinations of γ rays above the 10^+ state in the band. The high-energy part of the spectrum is displayed in the inset. (b) Spectrum of band 2 produced by summing many double-gated coincidence spectra. Peaks marked with a ''c'' are contaminant transitions. (c) Spectrum of band 3 produced in a similar manner as stated above. The high-energy transitions in the spectrum are shown in the inset.

Band 3 feeds both bands 1 and 2 as shown in Fig. 1, and a sample spectrum is shown in Fig. 2(c). Unfortunately, reliable DCO ratios could not be extracted for linking or in-band transitions of this sequence. Tentative spin assignments were made based on intensity, energy, and decay considerations. The parity of band 3 could not be determined based upon experimental information, but the possible configuration assignment (discussed below) suggests that the structure has positive parity.

A weak sequence, band 4 in Fig. 1, was observed to feed into band 1 at a high excitation energy. Once again, firm spin and parity assignments could not be made as DCO ratios could not be deduced. The tentative spin assignments for band 4 are based on the same arguments for the decay-out transitions as for band 2 and on intensity considerations (the former rules out the possibility of increasing the spins of

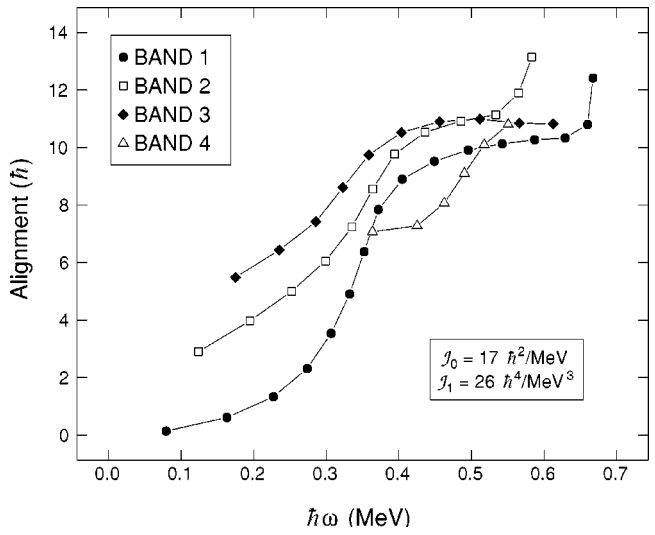

FIG. 3. Rotational alignments of bands 1–4 in ^{130}Nd. The Harris parameters of $\mathcal{J}_0 = 17\hbar^2/\mathrm{MeV}$ and $\mathcal{J}_1 = 26\hbar^4/\mathrm{MeV}^3$ were used to subtract the angular momentum of the collective core.

band 4 by $2\hbar$). The tentative negative-parity assignment is based on the arguments given in the next section.

IV. ROTATIONAL ALIGNMENTS AND CONFIGURATION ASSIGNMENTS

For a discussion of the ground-state band and the possible configurations of the linked side bands in ^{130}Nd, the rotational alignments of bands 1–4 are plotted in Fig. 3. Since comparisons with nearby nuclei are made, the commonly used Harris parameters [19] of $\mathcal{J}_0 = 17\hbar^2/\mathrm{MeV}$ and $\mathcal{J}_1 = 26\hbar^4/\mathrm{MeV}^3$ for this region (e.g. Refs. [14,20–22]) were employed to subtract the angular momentum of the collective core.

A large alignment gain of $\Delta i \approx 10\hbar$ at a crossing frequency of $\hbar\omega_c \approx 0.33$ MeV is observed for band 1. The only nucleons that can align at this low frequency and give such a large increase in alignment are the low-K $h_{11/2}$ protons. This proton alignment ($\mathrm{E}_p\mathrm{F}_p$) is well known in the mass 130 region and the crossing frequency and alignment gain are similar to those observed in nearby nuclei [23]. Cranked shell model (CSM) [24] calculations (using deformation parameters determined by TRS calculations) were performed for the quasiprotons and predicted the $\mathrm{E}_p\mathrm{F}_p$ crossing to be near $\hbar\omega = 0.35$ MeV, which is in good agreement with our experimental observations. A second crossing is expected in band 1 caused by the alignment of two $h_{11/2}$ quasineutrons (EF). The next indication for a crossing in band 1 is not found until very high frequencies (~ 0.66 MeV) in Fig. 3. However, the CSM quasineutron diagram shown in Fig. 4 indicates that the $h_{11/2}$ neutron alignment should occur near 0.5 MeV. (The alphabetic labeling of the quasineutron orbitals in Fig. 4 is summarized in Table II.) This is a 32% difference between the calculated and experimental values which is somewhat surprising since the CSM has predicted the EF crossing to within 10% of the observed frequency in several nearby nuclei [5,20,25]. At this time it is not clear why the expected EF alignment is significantly delayed in the ground-state band, however, a similar effect has been observed in the nearby Ce nuclei [21].

Band 2 has an initial alignment of approximately $3\hbar$ and gains $\sim 8\hbar$ of alignment near $\hbar\omega = 0.34$ MeV (see Fig. 3), which is associated with the $\mathrm{E}_p\mathrm{F}_p$ crossing. In the neighboring odd-Z isotones $^{129}_{59}$Pr [26] and $^{131}_{61}$Pm [22], the band based on an $h_{11/2}$ proton is found to be the yrast sequence. Therefore, the lowest lying two-quasiproton band in ^{130}Nd would likely have this proton in its configuration and would Pauli block the $\pi h_{11/2}$ crossing. Since this is not the case for band 2, a two-quasineutron configuration is a more reasonable

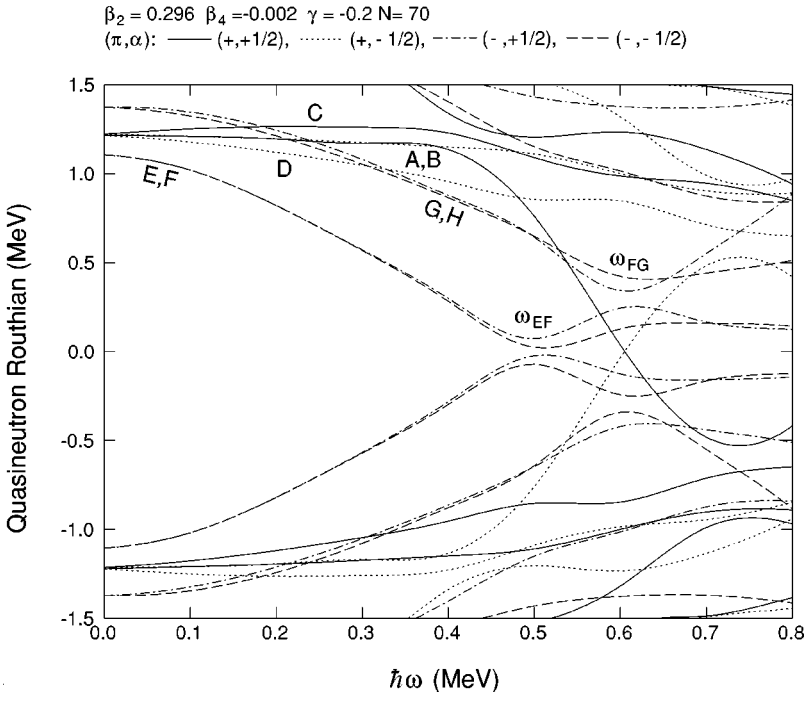

FIG. 4. Cranked shell model calculations for quasineutrons in ^{130}Nd. The deformation parameters (shown at the top of the figure) were determined by TRS calculations. Interpretation of the lines is displayed at the top of the figure. Explanation of the orbital labeling scheme is given in Table II.

TABLE II. Alphabetic quasiparticle labeling scheme for ^{130}Nd.

Label	$(\pi,\alpha)_n$ [a]	Configuration [b]	Label	$(\pi,\alpha)_n$ [a]	Configuration [b]
		Quasineutrons			
A	$(+,+\frac{1}{2})_1$	[402]5/2	B	$(+,-\frac{1}{2})_1$	[402]5/2
C	$(+,+\frac{1}{2})_2$	[411]1/2	D	$(+,-\frac{1}{2})_2$	[411]1/2
E	$(-,-\frac{1}{2})_1$	[523]7/2	F	$(-,+\frac{1}{2})_1$	[523]7/2
G	$(-,-\frac{1}{2})_2$	[541]1/2	H	$(-,+\frac{1}{2})_2$	[541]1/2

[a]Parity (π) and signature (α) of the orbital. The subscript n numbers the quasiparticle excitations of a specific signature and parity starting with the lowest in energy at $\hbar\omega=0$ MeV.
[b]Configuration of the orbital at $\hbar\omega=0$ MeV.

possibility. From an inspection of the band structures in the neighboring odd-N ^{129}Nd [27] and ^{131}Nd [20] nuclei, one concludes that the neutron orbitals $d_{5/2}[402]5/2$, $d_{3/2}/s_{1/2}[411]1/2$, $h_{11/2}[523]7/2$, and $h_{9/2}/f_{7/2}[541]1/2$ are all near the neutron Fermi surface for ^{130}Nd. Among those, the [523]7/2 band is the most intense structure in both odd-A nuclei suggesting that this neutron is a constituent of the lowest lying two-quasineutron configuration in ^{130}Nd. Therefore, band 2 likely has the E neutron in its configuration (the E configuration is systematically found to be more energetically favored than its signature partner F). Since E has a signature of $\alpha=-\frac{1}{2}$ and band 2 has been determined to have $\alpha=1$, the second quasineutron must also have negative signature, leaving B, D, and G as possibilities. To reduce the number of possible configurations, one can consider the additivity of alignment for these quasineutrons. The alignment values at $\hbar\omega=0.15$ MeV for the bands observed in ^{129,131}Nd are tabulated in Table III and the averages are displayed in the final column. By adding the average values for the E and G neutrons, one finds a larger alignment ($4.8\hbar$) than that observed for band 2 ($3.3\hbar$) at $\hbar\omega=0.15$ MeV. However, summing the average alignments of the E neutrons with either the B or D neutrons gives a value ($\sim 3.7\hbar$) close to that experimentally observed. Bands involving the [402]5/2 orbital are normally strongly coupled with little signature splitting, therefore, if the EB configuration is observed, one would expect to see it coupled with its EA signature partner. In contrast, large signature splitting is expected with the $\alpha=-\frac{1}{2}$ signature being favored for the [411]1/2 orbital (see Fig. 4). Thus we suggest that band 2 is the ED configuration, but we cannot completely rule out the EB assignment. A second crossing in band 2 can be observed in Fig. 3 at a frequency near 0.6 MeV. Perhaps this is the neutron crossing FG as the CSM predicts this alignment to occur at ~ 0.6 MeV (see Fig. 4).

Similar to bands 1 and 2, the alignment gain in band 3 at $\hbar\omega\approx 0.32$ MeV is attributed to the E_pF_p crossing. This implies that this latter structure is also a two-quasineutron band. From inspection of Fig. 3, one may notice that this sequence has a relatively high alignment value, $5.5\hbar$, at low frequency (<0.2 MeV). Only a combination of the [523]7/2 and [541]1/2 neutrons can produce such a large amount of initial alignment (see Table III). This has led to the positive-parity assignment of band 3 proposed in Fig. 1. Using the energetically favored signatures of these orbitals, E and H, respectively, one calculates from Table III an alignment value of $5.35\hbar$ (at 0.15 MeV) that is comparable to the experimental observation ($5.5\hbar$). The EH configuration would produce a sequence with signature $\alpha=0$, which is in agreement with the suggested spins for band 3 in Fig. 1. Thus we assign band 3 as the EH configuration.

Band 4 is a weak structure which is observed at high excitation energy. The initial alignment for this band is quite high, $\sim 7\hbar$, and one may notice from Fig. 3 that it apparently does not undergo the E_pF_p crossing. Both of these facts lead to the conclusion that band 4 is likely a two-quasiproton band where one of the protons is based on an $h_{11/2}$ orbital. A structure with an $h_{11/2}$ proton Pauli blocks the first proton crossing and has a high initial alignment, as the $\pi h_{11/2}$ bands in ^{129}Pr [26] and ^{131}Pm [22] have alignments of $\sim 4.5\hbar$ at low frequencies. Therefore, the configuration of band 4 is likely an $h_{11/2}$ proton coupled with a low-K $g_{7/2}$ or $d_{5/2}$ proton. Both of these positive-parity orbitals are found in neighboring odd-Z nuclei and have $\sim 1-2\,\hbar$ in initial alignment. The crossing at $\hbar\omega\approx 0.49$ MeV is attributed to either the $h_{11/2}$ neutron alignment (EF) or the second $h_{11/2}$ proton alignment (F_pG_p). The alignment gain of $\sim 4\hbar$ observed in band 4 is reasonable with either interpretation, and the CSM predicts crossing frequencies of 0.49 and 0.54 MeV for the neutron and proton crossings, respectively.

V. THE HIGHLY DEFORMED BAND

A regularly spaced ($\Delta E_\gamma\approx 70$ keV), weak sequence of γ rays has also been associated with ^{130}Nd. A spectrum of this rotational structure is shown in Fig. 5, where the inband transitions are designated with an asterisk. Although no link-

TABLE III. Rotational alignment values (units of $\hbar$) at frequency 0.15 MeV for different configurations in ^{129,131}Nd, based on experiments described in Refs. [20,27].

Configuration [a]	^{129}Nd	^{131}Nd	Average
A,B	1.2	1.0	1.1
C	1.1	0.7	0.9
D	1.6	1.2	1.4
E	2.4	2.4	2.4
F	2.4	2.2	2.3
G	2.4	2.4	2.4
H	3.0	2.9	2.95

[a]Configurations based on those summarized in Table II.

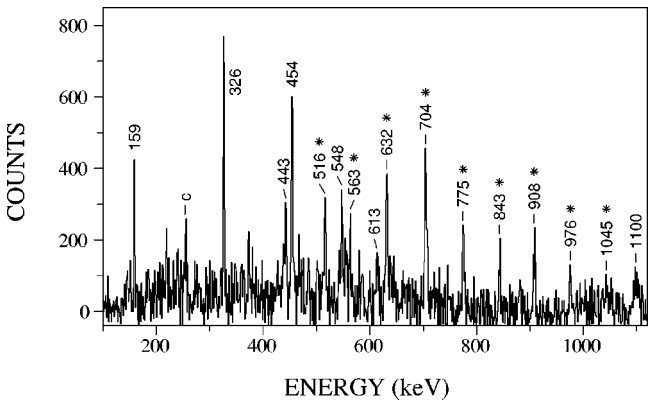

FIG. 5. Spectrum of the yrast highly deformed band in ^{130}Nd. The inband transitions are marked with an asterisk. The spectrum was produced by double-gating on all possible combinations of the inband transitions, except the 632 and 704 keV γ rays.

ing transitions could be identified from this band to any of the known bands in ^{130}Nd, the spectrum of this structure certainly indicates coincidence relationships with ground-state transitions of ^{130}Nd. Furthermore, the appearance of the 442.9 and 1100 keV transitions in the spectrum of Fig. 5 also indicates that it may feed band 2. Since the band could not be linked to known states, only an approximate spin assignment can be given. Transitions up to the 10^+ state of band 1 and γ rays depopulating the $9^{(-)}$ state in band 2 are seen in Fig. 5, which suggest that the spin of the lowest state is $I \geqslant 11$. The intensity of this sequence has been measured to be $\sim 0.5\%$ of the total population of the nucleus (as compared with similar structures in neighboring nuclei which are $\geqslant 2\%$).

Figure 6(a) displays the dynamical moments of inertia ($\mathcal{J}^{(2)}$) of all the bands in ^{130}Nd. The new rotational structure, labeled as band 5 in Fig. 6(a), has a nearly constant $\mathcal{J}^{(2)}$ just below $60\hbar^2$/MeV at frequencies above 0.3 MeV. This value is much larger than those for bands 1–4, whose $\mathcal{J}^{(2)} \approx 40\hbar^2$/MeV. In this region, a large constant dynamical moment of inertia is often associated with large deformation; therefore, we propose that band 5 is the yrast highly deformed band of ^{130}Nd. The configuration of the yrast highly deformed bands in Nd nuclei is commonly thought to be $\nu(i_{13/2}, h_{9/2})$ [28], as both orbitals are strongly downsloping in a single-particle diagram. Since structures based on these neutrons were recently observed in the odd-A neighboring ^{129,131}Nd [27,20] nuclei, both of these orbitals are near the Fermi surface of ^{130}Nd. Thus, the $\nu(i_{13/2}, h_{9/2})$ configuration appears to be a likely configuration assignment for this sequence in ^{130}Nd and a second minimum is indeed observed at $\beta_2 \approx 0.325$ for this configuration in TRS calculations.

The dynamical moments of inertia for the yrast highly deformed bands in the even-even ^{132,134,136}Nd [4,6,8] nuclei are plotted in Fig. 6(b) with the highly deformed band in ^{130}Nd. All of these bands are consistently near $60\hbar^2$/MeV between rotational frequencies of 0.4 and 0.5 MeV. However, below 0.4 MeV interactions appear in the bands of the three heavier nuclei, as indicated by the fluctuations in their $\mathcal{J}^{(2)}$ values. These interactions generally occur where the highly deformed bands decay out, which may be caused by

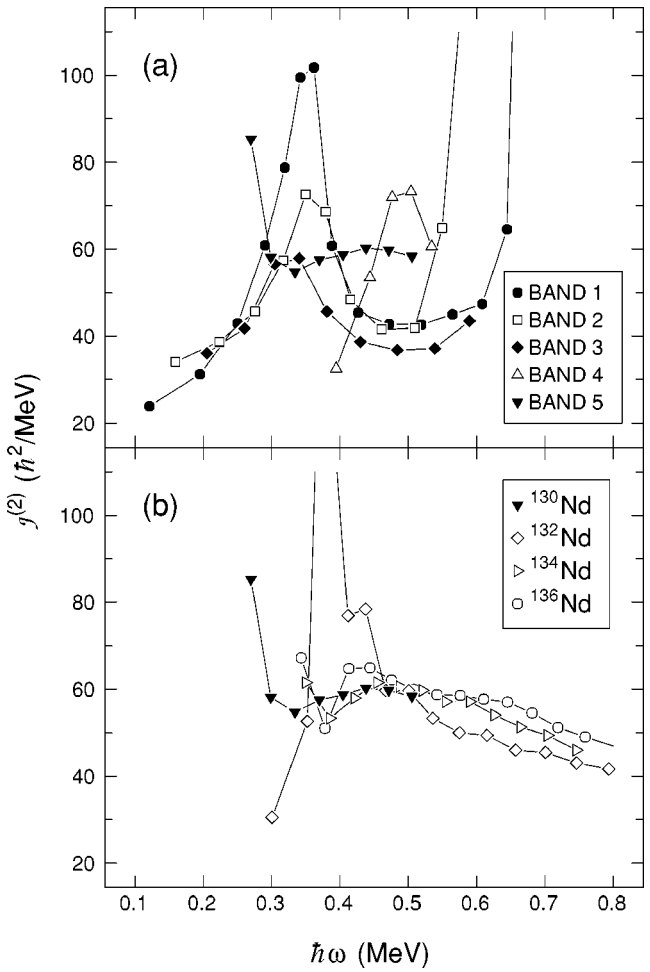

FIG. 6. Dynamical moments of inertia for (a) bands in ^{130}Nd and (b) the yrast highly deformed bands in ^{130,132,134,136}Nd.

mixing between the highly and normal deformed states [28]. As one can observe in Fig. 6(b), the structure in ^{130}Nd shows no interaction until ~ 0.25 MeV, suggesting that the intensity stays within the band to lower spins. As the neutron Fermi surface decreases to $N=70$ for ^{130}Nd, the $i_{13/2}$ and $h_{9/2}$ orbitals are likely lying increasingly higher in energy; therefore, the yrast highly deformed band lies higher in energy. The fact that this band is approximately five times weaker than the yrast highly deformed band in ^{132}Nd [4] also indicates that the band lies higher in energy in ^{130}Nd. The mixing between normal and highly deformed states in the heavier Nd nuclei occurs near spin $I \approx 17$, where the states are relatively close in energy. An interaction at this spin is less likely for ^{130}Nd since the highly deformed band may lie higher in energy, and therefore creates a larger energy difference between $I=17$ states. Instead, the decay to the normal deformed states occurs at a lower spin and thus the band can be observed to lower frequencies.

VI. SUMMARY

This investigation of high-spin states in ^{130}Nd has resulted in the extension of the ground-state band to higher spins and the establishment of three side bands. Based upon

their alignment behavior, configurations for these side bands have been proposed. A fifth band was also observed but could not be directly linked into the level scheme. This latter structure shows a large dynamical moment of inertia which is consistent with the yrast highly deformed bands observed in ^{132,134,136}Nd. Therefore, we suggest this fifth band is also highly deformed and it is observed to decay out at a lower frequency compared with the bands in the heavier Nd nuclei. The fact that the highly deformed band likely lies higher in energy could keep it from interacting with normal deformed states until lower spins.

ACKNOWLEDGMENTS

Special thanks to D. C. Radford for his software support and to the LBNL operations staff at Gammasphere. Discussions with D. L. Balabanski are gratefully acknowledged. This work is funded by the U.S. Department of Energy through Contract Nos. DE-FG02-96ER40983 (University of Tennessee) and DE-FG05-88ER40406 (Washington University). ORNL is managed by UT-Battelle, LLC, for the U.S. DOE under Contract No. DE-AC05-00OR22725.

[1] R.M. Clark, I.Y. Lee, P. Fallon, D.T. Joss, S.J. Asztalos, J.A. Becker, L. Bernstein, B. Cederwall, M.A. Delaplanque, R.M. Diamond, L.P. Farris, K. Hauschild, W.H. Kelly, A.O. Macchiavelli, P.J. Nolan, N. O'Brien, A.T. Semple, F.S. Stephens, and R. Wadsworth, Phys. Rev. Lett. **76**, 3510 (1996).

[2] F.G. Kondev, M.A. Riley, D.J. Hartley, T.B. Brown, R.W. Laird, M. Lively, R.K. Sheline, E.S. Paul, D.T. Joss, P.J. Nolan, S.L. Shepherd, R.M. Clark, P. Fallon, D.G. Sarantites, M. Devlin, D.R. LaFosse, F. Lerma, R. Wadsworth, I.M. Hibbert, N.J. O'Brien, and J. Simpson, Phys. Rev. C **60**, 011303(R) (1999).

[3] D.J. Hartley, W. Reviol, L.L. Riedinger, F.G. Kondev, A. Galindo-Uribarri, D.G. Sarantites, H.Q. Jin, D.R. LaFosse, S.M. Mullins, B.H. Smith, and J.N. Wilson, Phys. Rev. C **60**, 041301(R) (1999).

[4] C.M. Petrache, D. Bazzacco, P. Bednarczyk, G. de Angelis, M. DePoli, C. Fahlander, G. Falconi, E. Farnea, A. Gadea, M. Lunardon, S. Lunardi, N. Marginean, R. Menegazzo, P. Pavan, Zs. Podolyák, C. Rossi Alvarez, C.A. Ur, R. Venturelli, L.H. Zhu, and R. Wyss, Phys. Lett. B **415**, 223 (1997).

[5] D. Bazzacco, F. Brandolini, G. Falconi, S. Lunardi, N.H. Medina, P. Pavan, C. Rossi-Alvarez, G. de Angelis, D. De Acuna, M. De Poli, D.R. Napoli, J. Rico, D. Bucurescu, M. Ionescu-Bujor, and C.A. Ur, Phys. Rev. C **58**, 2002 (1998).

[6] C.M. Petrache, D. Bazzacco, S. Lunardi, C. Rossi Alvarez, R. Venturelli, R. Burch, P. Pavan, G. Maron, D.R. Napoli, L.H. Zhu, and R. Wyss, Phys. Lett. B **387**, 31 (1996).

[7] E.M. Beck, F.S. Stephens, J.C. Bacelar, M.A. Delaplanque, R.M. Diamond, J.E. Draper, C. Duyar, and R.J. McDonald, Phys. Rev. Lett. **58**, 2182 (1987).

[8] C.M. Petrache, D. Bazzacco, S. Lunardi, C. Rossi Alvarez, R. Venturelli, D. Bucurescu, C.A. Ur, D. De Acuna, G. Maron, D.R. Napoli, N.H. Medina, J.R.B. Oliveira, and R. Wyss, Phys. Lett. B **373**, 275 (1996).

[9] R. Wadsworth, A. Kirwan, D.J.G. Love, Y.-X. Luo, J.-Q. Zhong, P.J. Nolan, P.J. Bishop, M.J. Godfrey, R. Hughes, A.N. James, I. Jenkins, S.M. Mullins, J. Simpson, D.J. Thornley, and K.L. Ying, J. Phys. G **13**, L207 (1987).

[10] P. Möller and J.R. Nix, At. Data Nucl. Data Tables **59**, 185 (1995).

[11] R. Janssens and F. Stephens, Nucl. Phys. News **6**, 9 (1996).

[12] D.G. Sarantites, P.-F. Hua, M. Devlin, L.G. Sobotka, J. Elson, J.T. Hood, D.R. LaFosse, J.E. Sarantites, and M.R. Maier, Nucl. Instrum. Methods Phys. Res. A **381**, 418 (1996).

[13] D.C. Radford, Nucl. Instrum. Methods Phys. Res. A **361**, 297 (1995).

[14] R. Wadsworth, P. Regan, S.M. Mullins, G.J. Gyapong, D.L. Watson, P.J. Nolan, M.J. Godfrey, I. Jenkins, Y.J. He, B.J. Varley, J. Simpson, and W. Gelletly, Z. Phys. A **333**, 411 (1989).

[15] L. Grodzins, Phys. Lett. **2**, 88 (1962).

[16] S. Raman, C.W. Nestor, and K.H. Bhatt, Phys. Rev. C **37**, 805 (1988).

[17] R. Wyss, J. Nyberg, A. Johnson, R. Bengtsson, and W. Nazarewicz, Phys. Lett. B **215**, 211 (1988).

[18] R. Wadsworth, S.M. Mullins, J.R. Hughes, P.J. Nolan, A. Kirwan, P.J. Bishop, I. Jenkins, M.J. Godfrey, and D.J. Thornley, J. Phys. G **15**, L47 (1989).

[19] S.M. Harris, Phys. Rev. **138**, B509 (1965).

[20] D.J. Hartley, W. Reviol, L.L. Riedinger, D.L. Balabanski, H.Q. Jin, B.H. Smith, O. Zeidan, Jing-ye Zhang, A. Galindo-Uribarri, D.G. Sarantitesb, D.R. LaFosse, J.N. Wilson, and S.M. Mullins, Phys. Rev. C **61**, 044328 (2000).

[21] E.S. Paul, P. Bednarczyk, A.J. Boston, C.J. Chiara, C. Foin, D.B. Fossan, J. Genevey, A. Gizon, J. Gizon, D.G. Jenkins, N. Kelsall, N. Kintz, T. Koike, D.R. LaFosse, P.J. Nolan, B.M. Nyakó, C.M. Parry, J.A. Sampson, A.T. Semple, K. Starosta, J. Timár, R. Wadsworth, A.N. Wilson, and L. Zolnai, Nucl. Phys. **A676**, 32 (2000).

[22] C.M. Parry, A.J. Boston, C. Chandler, A. Galindo-Uribarri, I.M. Hibbert, V.P. Janzen, D.T. Joss, S.M. Mullins, P.J. Nolan, E.S. Paul, P.H. Regan, S.M. Vincent, R. Wadsworth, D. Ward, and R. Wyss, Phys. Rev. C **57**, 2215 (1998).

[23] D.J. Hartley, L.L. Riedinger, H.Q. Jin, W. Reviol, B.H. Smith, A. Galindo-Uribarri, D.G. Sarantites, D.R. LaFosse, J.N. Wilson, and S.M. Mullins, Phys. Rev. C **60**, 014308 (1999).

[24] R. Bengtsson and S. Frauendorf, Nucl. Phys. **A327**, 139 (1979); **A314**, 27 (1979).

[25] D. Ward, V.P. Janzen, H.R. Andrews, D.C. Radford, G.C. Ball, D. Horn, J.C. Waddington, J.K. Johansson, F. Banville, J. Gascon, S. Monaro, N. Nadon, S. Pilotte, D. Prevost, P. Taras, and R. Wyss, Nucl. Phys. **A529**, 315 (1991).

[26] A. Galindo-Uribarri *et al.*, Atomic Energy of Canada Ltd., AECL-11132 PR-TASCC-09 3.1.15, 1994.

[27] O. Zeidan (private communication).

[28] C.M. Petrache, D. Bazzacco, G. Falconi, S. Lunardi, E. Maglione, R. Menegazzo, C. Rossi Alvarez, R. Venturelli, G. Viesti, G. de Angelis, M. De Poli, C. Fahlander, E. Farnea, A. Gadea,

G. Maron, D.R. Napoli, Zs. Podolyàk, S. Perriès, A. Astier, L. Ducroux, M. Meyer, N. Redon, A. Bracco, S. Frattini, S. Leoni, I. Deloncle, M.G. Porquet, N. Marginean, C.A. Ur, B. Cederwall, A. Johnson, and R. Wyss, in *Nuclear Structure 98*, edited by C. Baktash, AIP Conf. Proc. No. 481 (AIP, Woodbury, NY, 1999), p. 368.